

**Conductance of a photochromic molecular switch with graphene leads**

C. Motta\*

*Dipartimento di Scienza dei Materiali and Corimav Pirelli, Università di Milano-Bicocca, via Cozzi 53, IT-20125 Milano, Italy*

M. I. Trioni

*CNR - National Research Council of Italy, ISTM, Via Golgi 19, IT-20133 Milano, Italy*

G. P. Brivio

*CNISM, ETSF, and Dipartimento di Scienza dei Materiali, Università di Milano-Bicocca, via Cozzi 53, IT-20125 Milano, Italy*

K. L. Sebastian

*Department of Inorganic and Physical Chemistry, Indian Institute of Science, Bangalore, India*

(Received 24 June 2011; revised manuscript received 12 August 2011; published 19 September 2011)

We report a full self-consistent *ab initio* calculation of the conductance of a diarylethene-based molecular switch with two graphene electrodes. Our results show the contributions of the resonant states of the molecule, of the electrode density of states, and of graphene unique features, such as edge states. The conductivities are found to be significantly different for the two photochromic isomers at zero and finite applied bias. Further we point out the possibility of causing the switching by the application of a large potential difference between the two electrodes.

DOI: [10.1103/PhysRevB.84.113408](https://doi.org/10.1103/PhysRevB.84.113408)

PACS number(s): 73.23.-b, 73.40.-c, 72.80.Vp

**I. INTRODUCTION**

Organic electronics has rapidly grown into a fundamental field whose potential is still to be fully developed and exploited. Research focuses on novel functional organic materials and existing applications already comprise, among others, nanoscale electronic devices, such as thin film transistors and diodes, solar cells, integrated circuits on flexible substrates, carbon nanotube field effect transistors, and molecular switches. A promising class of organic molecular-scale photoswitching units is provided by photochromic molecules which are able to switch between two chemical structures when irradiated by light of appropriate wavelengths. Such configurations correspond to photochemically interconvertible isomers.<sup>1</sup>

A recently developed class of molecules, named diarylethenes, displays a photochromic, thermally irreversible, reactivity.<sup>2,3</sup> Most of them exhibit light induced switching both in solution and in single crystals<sup>2,4,5</sup> by changing reversibly in aromaticity during the closed-open (open-closed) configuration transition, induced by visible and ultraviolet light, respectively.<sup>6</sup> This property raised much interest and stimulated research on diarylethene derivatives as suitable photochromic molecular switches.<sup>7,8</sup> Investigations of diarylethene junctions with gold electrodes showed that conductivity is larger by two orders of magnitude in the closed isomer in comparison with that of the open one.<sup>9</sup> Nonetheless several diarylethene derivatives on gold leads only display photochromic switching from the closed to the open state after irradiation with visible light but not the reverse process by UV<sup>10,11</sup> owing to the fast quenching of the photoexcited hole of the highest occupied molecular orbital (HOMO) state of the open isomer by the gold electrodes.<sup>12</sup> By connecting the metal anchoring sulfur atom through a phenyl group spacer, reversible light-induced switching resulted both on Au(111)<sup>13</sup> and gold nanoparticles.<sup>14</sup>

Photochromic diarylethene derivatives are also investigated on single walled carbon nanotubes (SWCNT) as perspective single molecule devices with more accurately defined contacts to the electrodes.<sup>15</sup> For such systems it was found that switching from insulating to conducting, i.e., from an open to a closed molecular configuration, occurs, but not the reverse, unlike in the case of Au.<sup>16</sup> The timely character of this topic is evidenced by the wealth of theoretical studies on the conductance of photochromic switches both with gold<sup>3,12,17-21</sup> and SWCNT electrodes.<sup>22</sup>

In this paper we investigate the conductance of a diarylethene switch sandwiched between two semi-infinite graphene electrodes by the Landauer formalism recast in terms of the nonequilibrium Green function (NEGF) within the density functional theory (DFT).<sup>23</sup> In fact, the two-dimensional (2D) form of carbon has just revealed several intriguing fundamental properties and a huge potential for applications in nanoelectronics. In particular, high chemical stability, low resistivity, and mechanical strength suggest graphene, a more cost-effective material than carbon nanotubes, as an alternative component for electrodes in electronic devices.<sup>24</sup> Furthermore in graphene electrons can travel ballistically up to a micrometer,<sup>25</sup> as electron-phonon scattering is very weak.<sup>26</sup> This implies a carrier mobility larger than that of the inorganic semiconductor with the largest mobility, i.e., InSb, and that of carbon nanotubes. If defects and impurities are eliminated, such mobility is about  $2 \times 10^5$  cm<sup>2</sup>/Vs,<sup>25</sup> but in practice graphene sheets have irregular shapes and contain impurities and defects. To overcome this difficulty we point out a promising bottom-up experimental technique capable of synthesizing graphene starting from small corene blocks and building well defined molecule electrode contacts.<sup>27</sup> Transparent, conductive, and ultrathin graphene films have been demonstrated to be an alternative to metal-oxide electrodes for solid-state dye-sensitized solar cells.<sup>28</sup>

Our calculations show that at zero bias the peaks in conductance of the diarylethene moiety attached to two graphene electrodes reflect not only the molecule electronic states broadened into resonances by the coupling to the leads, but also the features of graphene edge states. Near the Fermi energy ( $E_F$ ) the conductance of the closed isomer is much lower in the energy interval between the HOMO and the lowest unoccupied molecular orbital (LUMO) resonances of the molecule, following the linear dependence of the electrode density of states (DOS) proportional to  $|E - E_F|$ . In the same range the conductance of the open isomer is almost zero. If we apply a finite bias, we observe that conductance is allowed within different energy windows for the open and closed isomers.

In Sec. II we outline the calculation model and the method. Sections III and IV are devoted to the presentation of results and their discussion and to conclusions, respectively.

## II. MODEL AND METHODS

We studied the open and closed structures of two different diarylethene molecules, shown in Fig. 1. The central dithienylethene part is the same for each molecule, and it is attached to the electrodes through  $-R-$  with  $R = \text{CH}_2$  (we call this A1) and  $R = \text{CO}-\text{NH}$  (referred to as A2). We also considered longer isomers, which have two phenyl linkers and are connected in the same fashion, namely B1 and B2. We started with optimized structures of the molecules with the two R groups connected to H atoms. Then the two H atoms were removed and the molecules were embedded between the two graphene sheets. The graphene electrodes were taken to have zig-zag edges with the valencies of the edge C atoms satisfied by H atoms. We did this because C atoms at zig-zag terminations display stronger affinity toward radicals, and hence form stronger bonds with H atoms. Graphene with zig-zag edges has a unique edge state near the Fermi level.<sup>29</sup> These are states for which the wave functions are localized in the edge and have been discussed in detail by Nakada *et al.*<sup>30</sup> In comparison the armchair edge has no such localized state. Further, we also optimized the energy by varying the electrode-electrode distance. We remark that in the optimized geometry, the plane of the molecule is approximately perpendicular to the

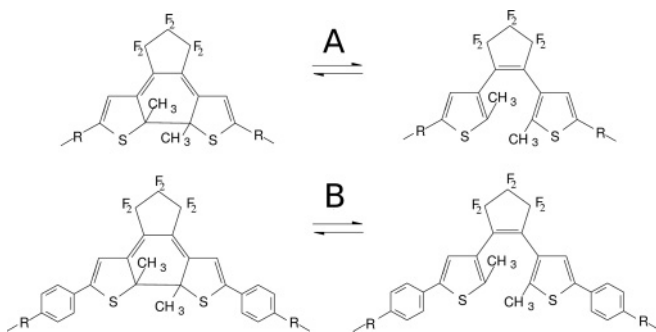


FIG. 1. Structures of the closed and open forms of the two diarylethene derivatives studied in this work. Here, R is the functional group that links the molecule to graphene, which is  $-\text{CH}_2-$  in the first case (A1 and B1) and  $-\text{CO}-\text{NH}-$  (amide linking) in the second case (A2 and B2).

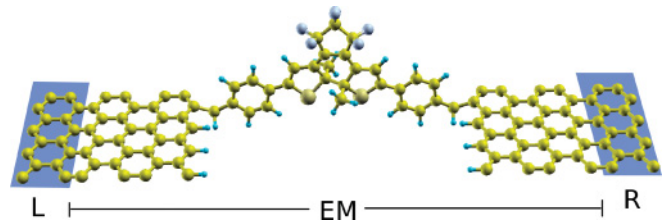


FIG. 2. (Color online) Geometry setup for the conductance calculations.

plane of the two graphene sheets. This minimizes the coupling of  $\pi$  states of the molecule with those of graphene, which can be advantageous in certain cases. In fact, it would be interesting to tune the orientation of the molecular plane with respect to that of graphene by linking the molecule to more than one carbon of the graphene. In this way, one could adjust the hybridization of the molecular levels by changing the relative orientation of the molecule with respect to the graphene plane.

The system may thus be thought of as comprised of three separate parts: the left (L) and right (R) semi-infinite graphene leads, and an extended molecule (EM) region, as reported in Fig. 2. For each electrode, six layers of carbon atoms are included in the EM region in order to screen the perturbation from the central region. With this, the final geometry with the contacts is relaxed again. The graphene electrodes are constructed so that the periodic replicas of the contact region are separated by four unit cells (i.e., 7.436 Å), and the interaction among them is negligible. Our electronic structure calculations are carried out using the DFT self-consistent pseudopotential method implemented in SIESTA package.<sup>31</sup> The exchange-correlation effect and electron-ion interaction are described by the Perdew-Burke-Ernzerhof generalized gradient approximation and the norm-conserving pseudopotential in the fully nonlocal form, respectively. A double- $\zeta$  plus polarization basis set accounts for the localized atomic orbitals and an energy cutoff for real space mesh size is set to be 200 Ry. The positions of carbon atoms are the ideal positions of a previously relaxed graphene sheet, while the hydrogen positions are relaxed for each junction. We performed all relaxations with a force tolerance of 0.04 eV/Å. For the self-consistent calculations, 12 K points are used in the transversal direction (that of the electrode's edge) while for the calculations of the transmission function, 60 K points are taken into account. The vacuum portions between two neighboring graphene sheets are set to be 15 Å.

The transmission function of the system is calculated by the TRANSIESTA code<sup>32</sup> which combines the NEGF technique with the DFT. The transmission function  $T(E, V)$  can be obtained by the following equation:

$$T(E, V) = \text{Tr}[\Gamma_L(E)G(E, V)\Gamma_R(E)G^\dagger(E, V)], \quad (1)$$

where the spectral density  $\Gamma_{L(R)}$  describes the coupling between the L (R) electrode and the EM region, and it is given by the imaginary part of the electrode self-energy:  $\Gamma_{L(R)}(E) = i(\Sigma_{L(R)} - \Sigma_{L(R)}^\dagger)$ . The self-energies describe the hopping between the L (R) lead and the EM region by establishing the appropriate boundary conditions for the Green

function calculation.  $G$  is the retarded Green function of the EM region, formally given by

$$G(E, V) = [ES - H(V) - \Sigma_L(E) - \Sigma_R(E)]^{-1}, \quad (2)$$

where  $S$  is the overlap matrix and  $H$  is the Hamiltonian of the system when a bias voltage  $V$  is applied. The current is simply given by the following integral:

$$I(V) = \frac{2e}{h} \int_{-\infty}^{\infty} dE T(E, V) [f(E - \mu_L) - f(E - \mu_R)], \quad (3)$$

with  $f$  being the occupation Fermi function and  $\mu_{L(R)}$  the chemical potential of the L (R) electrode.

Our calculations are performed at absolute zero temperature. The results are similar for the four molecules shown in Fig. 1, and we choose to discuss those of B1 in depth.

### III. RESULTS AND DISCUSSION

In the upper panels of Fig. 3, we present the total DOS (solid line) of the extended system and the projected density of states (PDOS) (shaded area) onto the molecular region, as function of the electron energy, the left and the right one for the closed and open isomer, respectively. The transmission function dependence on the injected electron energy is shown in logarithmic scale in the lower panels of Fig. 3. The total DOS is reminiscent of that of the electrodes, since near  $E_F$  it displays a linear dispersion following that of an ideal, infinite graphene sheet. Of course, very close to  $E_F$  the dispersion is not perfectly linear due to the existence of a vacuum region between two graphene sheets. Furthermore we remark the presence of two low peaks very near  $E_F$ , one slightly above and the other just below it. They are states mainly localized at the molecule-electrode interface whose origin stems from the zig-zag termination edge states of the two graphene sheets interacting with the orbitals of the molecule in the coupled system. We point out that, as a consequence of the perturbation due to the junction, such states lie within the continuum graphene spectrum, and they become resonant conducting states, which do not exist in SWCNT.<sup>27</sup> Apart

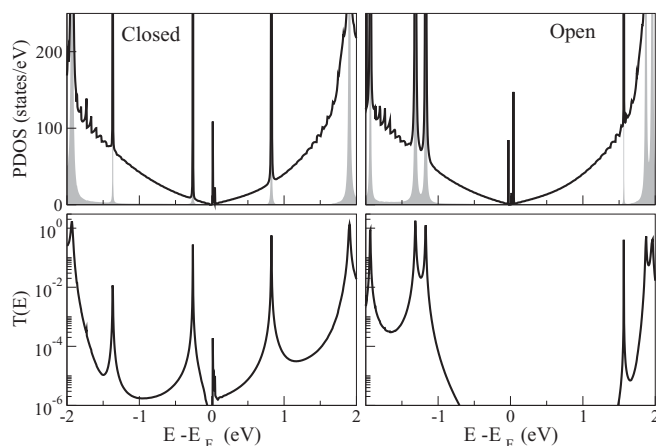


FIG. 3. PDOS and transmission function for the closed (left) and open (right) isomers of B1 diarylethene. Upper panel: DOS (line) and PDOS (shaded area) on the molecular region. Lower panels: zero-bias transmission functions.

from the edge states, all peaks in the PDOS refer to molecular orbitals broadened by the interaction with the electrodes and a corresponding feature at the same energy appears in the transmission function. We concentrate on the two main peaks of conductance for each isomer that appear on the left and on the right side of  $E_F$ . They are due to the hybridization of the HOMO and LUMO states of the molecule with the graphene substrate. For the closed isomer such states are closer to  $E_F$ , and their intensity is lower, if compared with most of other molecular resonances, since the DOS of the underlying graphene sheets tends to zero as the energy approaches  $E_F$ . However, considering small enough energy deviations from  $E_F$ , the transmission function is always larger for the closed isomers than for the open ones. The lower conductance of the open isomers is due to their distorted geometry: the breaking of the central C–C bond due to the closed-open transition affects the  $\pi$  conjugation of the structure, reducing it.<sup>33</sup> Hence, the electrons are less delocalized along the molecular backbone, reducing transmission. In Fig. 4 we display the real part of the wave functions for three representative states of the system, namely the LUMO of the closed isomer, the LUMO of the open isomer, and one edge state of the open molecule. We observe that the former LUMO is more widely spread than the latter one, reflecting its more extended  $\pi$  conjugation. The plotted edge state shows a rapid decay inside the molecular region. The other edge state just mirrors it on the opposite side of the junction. Comparing the transmission functions of diarylethene with different connecting groups (B1 and B2), we noticed that the presence of the amide end groups in the latter molecule produces a slight shift of the peaks toward higher energies. This results in a better alignment of the HOMO of the closed isomer with  $E_F$  so, once a voltage is applied, a larger current may be obtained in this case. Apart from this shift, the structure of the transmission function is not appreciably affected by the change of connecting groups.

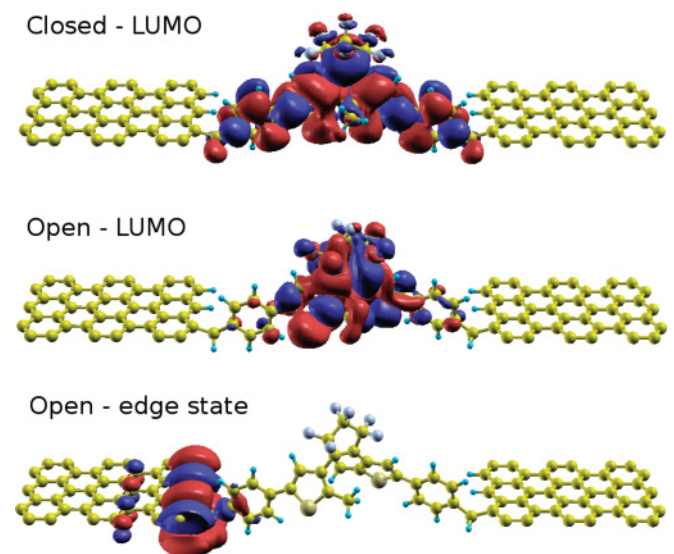


FIG. 4. (Color online) Real part of some representative wave functions of the junction with molecule B1: the LUMO of the closed isomer (upper panel), the LUMO of the open isomer (middle panel), and one edge state for the open isomer (lower panel).

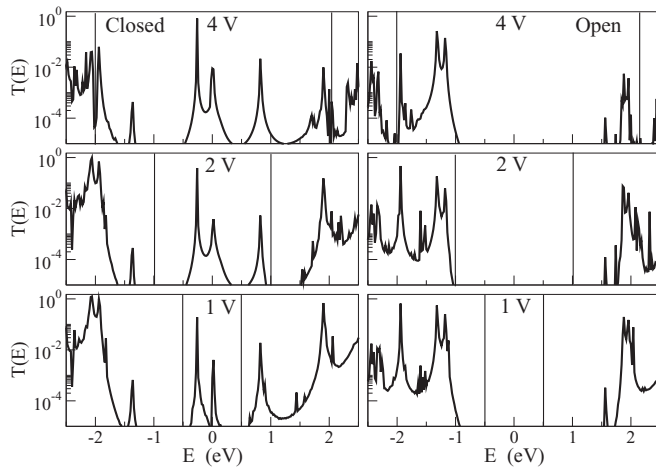


FIG. 5. Transmission function of the closed (left) and open (right) isomers of the B1 diarylethene derivative at different applied biases (from bottom to top: 1V, 2V, and 4V). The bias window is delimited by two vertical lines. The energy scale is referred to the average value of the left and right chemical potentials  $(\mu_L - \mu_R)/2$ .

We now discuss the changes in the conductance for molecule B1 when the system is driven out of equilibrium by the application of a bias  $V$ . In Fig. 5 the transmission functions are reported for the closed (left panel) and open isomer (right panel) for three different values of  $V$ . For the closed molecule a bias of 1 V allows one to include the contribution of the HOMO in the admissible energy window (vertical lines), while a bias of 2 V is needed to contain the LUMO. We also observe a feature very close to  $E = 0$  which is due to the superposition of two narrow resonances arising from the edge states. In fact, as a finite bias is applied, edge states play a role, though small, in the transmission curve. A nonnegligible conductance asks for a bias  $V = 4$  V for the open isomer. In both cases the HOMO-LUMO energy difference is unaffected by the applied voltage.

In solution, diarylethene-based molecules can be switched between the two states by photochemical means. When used as a bridge between two Au electrodes, the switching occurs, usually in one direction only, due to quenching by the electrodes. For CNT electrodes too, the switching from open

to closed isomers occurs through light, but the reverse does not.<sup>16</sup> We suggest the use of graphene as the electrode as (1) it has a lower density of states near the Fermi level in comparison with Au leading to lesser probability for quenching and (2) the orientation of the molecule with respect to the graphene sheet can be changed chemically, tuning the interaction between the two components. In the polymeric state, the change from the closed state to the open state can be induced not only by light, but also by electron/hole injection obtained by the application of a potential difference.<sup>3</sup> Consequently one may anticipate that in the case of diarylethene molecules connected to graphene, the switching from open to closed may be induced by light and the reverse by the application of a large potential difference. One has the possibility of inducing switching in both directions by the application of such a potential difference for a short period of time, and hence light may be avoided altogether. In fact, looking at the positions of the LUMO/HOMO orbitals energies in the transmission curves given in Fig. 5, it seems possible to populate/depopulate them to a sizable extent by the application of about 2 and 4 V for the closed and open configurations, respectively.

#### IV. CONCLUSIONS

In conclusion we have calculated the conductance of the two isomers of diarylethene-based molecules and analyzed the role of the graphene leads. We have analyzed the transmission function for the open and closed isomers both at zero and finite applied bias, pointing out the role of graphene surface edge states. We have discussed the advantages of using graphene electrodes with respect to other materials, namely, a reduced quenching of the photoexcited state compared to gold electrodes and the possibility to tune the resonant HOMO and LUMO hybridization by changing the orientation of the molecule with respect to the leads plane. We also stress that in the case of graphene, the switch can be operated electrically by the application of short pulses, making it potentially very useful, in comparison with other electrodes.

#### ACKNOWLEDGMENT

C. M. and K. L. S. thank CARIPLO Foundation for its support within the PCAM European Doctoral Programme.

\*c.motta10@campus.unimib.it

<sup>1</sup>M. Irie, T. Fukaminato, T. Sasaki, N. Tamai, and T. Kawai, *Nature (London)* **420**, 759 (2002).

<sup>2</sup>M. Irie, *Proc. Jpn. Acad. Ser. B-Phys. Biol. Sci.* **86**, 472 (2010).

<sup>3</sup>S. Nakamura, S. Yokojima, K. Uchida, T. Tsujioka, A. Goldberg, A. Murakami, K. Shinoda, M. Mikami, T. Kobayashi, and S. Kobatake, *J. Photochem. Photobiol., A* **200**, 10 (2008).

<sup>4</sup>M. Irie, S. Kobatake, and H. Horichi, *Science* **291**, 1769 (2001).

<sup>5</sup>S. Kobatake, S. Takami, H. Muto, T. Ishikawa, and M. Irie, *Nature (London)* **446**, 778 (2007).

<sup>6</sup>J. Huang, Q. Li, H. Su, and J. Yang, *Chem. Phys. Lett.* **479**, 120 (2009).

<sup>7</sup>N. Katsonis, M. Lubomska, M. M. Pollard, B. L. Feringa, and P. Rudolf, *Prog. Surf. Sci.* **82**, 407 (2007).

<sup>8</sup>S. J. van der Molen and P. Liljeroth, *J. Phys. Condens. Matter* **22**, 133001 (2010).

<sup>9</sup>J. He, F. Chen, P. A. Liddell, J. Andréasson, S. D. Straight, D. Gust, T. A. Moore, A. L. Moore, J. Li, O. F. Sankey, and S. M. Lindsay, *Nanotechnology* **16**, 695 (2005).

<sup>10</sup>D. Dulic, S. J. van der Molen, T. Kudernac, H. T. Jonkman, J. J. D. de Jong, T. N. Bowden, J. van Esch, B. L. Feringa, and B. J. van Wees, *Phys. Rev. Lett.* **91**, 207402 (2003).

- <sup>11</sup>S. J. van der Molen, H. van der Vegte, T. Kudernac, I. Amin, B. L. Feringa, and B. J. van Wees, *Nanotechnology* **17**, 310 (2006).
- <sup>12</sup>J. Li, G. Speyer, and O. F. Sankey, *Phys. Rev. Lett.* **93**, 248302 (2004).
- <sup>13</sup>N. Katsonis, T. Kudernac, M. Walko, S. J. van der Molen, B. J. van Wees, and B. L. Feringa, *Adv. Mater.* **18**, 1397 (2006).
- <sup>14</sup>T. Kudernac, S. J. van der Molen, B. J. van Wees, and B. L. Feringa, *Chem. Commun.* 3597 (2006).
- <sup>15</sup>X. Guo, J. P. Small, J. E. Klare, Y. Wang, M. S. Purewal, I. W. Tam, B. H. Hong, R. Caldwell, L. Huang, S. O'Brien, J. Yan, R. Breslow, S. Wind, J. Hone, P. Kim, and C. Nuckolls, *Science* **311**, 356 (2006).
- <sup>16</sup>A. C. Whalley, M. L. Steigerwald, X. Guo, and C. Nuckolls, *J. Am. Chem. Soc.* **129**, 12590 (2007).
- <sup>17</sup>M. Kondo, T. Tada, and K. Yoshizawa, *Chem. Phys. Lett.* **412**, 55 (2005).
- <sup>18</sup>J. Huang, Q. Li, H. Ren, H. Su, Q. W. Shi, and J. Yang, *J. Chem. Phys.* **127**, 094705 (2007).
- <sup>19</sup>A. Staykov, D. Nozaki, and K. Yoshizawa, *J. Phys. Chem. C* **111**, 3517 (2007).
- <sup>20</sup>S. Ying Quek, M. Kamenetska, M. L. Steigerwald, H. J. Choi, G. Louie, M. S. Hybertsen, J. B. Neaton, and L. Venkataraman, *Nat. Nanotech.* **4**, 230 (2009).
- <sup>21</sup>A. Odell, A. Delin, B. Johansson, I. Rungger, and S. Sanvito, *ACS Nano* **4**, 2635 (2010).
- <sup>22</sup>P. Zhao, P. Wang, Z. Zhang, C. Fang, Y. Wang, Y. Zhai, and D. Liu, *Solid State Commun.* **149**, 928 (2009).
- <sup>23</sup>S. Datta, *Electronic Transport in Mesoscopic Systems* (Cambridge University Press, Cambridge, United Kingdom, 1995).
- <sup>24</sup>S. Pang, H. N. Tsao, L. Feng, and K. Muellen, *Adv. Mater.* **21**, 3488 (2009).
- <sup>25</sup>J. H. Chen, C. Jang, S. Xiao, M. Ishigami, and M. S. Fuhrer, *Nat. Nanotech.* **3**, 206 (2008).
- <sup>26</sup>S. V. Morozov, K. S. Novoselov, M. I. Katsnelson, F. Schedin, D. C. Elias, J. A. Jaszczak, and A. K. Geim, *Phys. Rev. Lett.* **100**, 016602 (2008).
- <sup>27</sup>I. Diez-Perez, Z. Li, J. Hihath, J. Li, C. Zhang, X. Yang, L. Zang, Y. Dai, X. Feng, K. Muellen, and N. Tao, *Nat. Commun.* **1**, 31 (2010).
- <sup>28</sup>X. Wang, L. Zhi, and K. Mullen, *Nano Lett.* **8**, 323 (2008).
- <sup>29</sup>D. J. Jiang, B. G. Sumpter, and S. Dai, *J. Chem. Phys.* **126**, 134701 (2007).
- <sup>30</sup>K. Nakada, M. Fujita, G. Dresselhaus, and M. S. Dresselhaus, *Phys. Rev. B* **54**, 17954 (1996).
- <sup>31</sup>J. M. Soler, E. Artacho, J. D. Gale, A. Garcia, J. Junquera, P. Ordejón, and D. Sanchez-Portal, *J. Phys. Condens. Matter* **14**, 22 (2001).
- <sup>32</sup>M. Brandbyge, J. L. Mozos, P. Ordejón, J. Taylor, and K. Stokbro, *Phys. Rev. B* **65**, 165401 (2002).
- <sup>33</sup>M. J. Marsella, Z. Wang, and R. H. Mitchell, *Org. Lett.* **2**, 2979 (2000).